УДК 532.526.4

ТЕОРИЯ ТУРБУЛЕНТНОСТИ И МОДЕЛИРОВАНИЕ ТУРБУЛЕНТНОГО ПЕРЕНОСА В АТМОСФЕРЕ ЧАСТЬ 6

Трунев Александр Петрович
к. ф.-м. н., Ph.D.
Директор, *A&E Trounev IT Consulting, Торонто, Канада*

Дана модель непрерывного перехода от ламинарного к турбулентному течению в пограничном слое. Развита теория спектральной плотности турбулентных пульсаций

Ключевые слова: АТМОСФЕРНАЯ ТУРБУЛЕНТНОСТЬ, ТУРБУЛЕНТНЫЙ ПЕРЕНОС, УСКОРЕННЫЕ ТЕЧЕНИЯ, ПОГРАНИЧНЫЙ СЛОЙ, ШЕРОХОВАТАЯ ПОВЕРХНОСТЬ, ПРИЗЕМНЫЙ СЛОЙ АТМОСФЕРЫ, ТУРБУЛЕНТНЫЙ ПЕРЕНОС АЭРОЗОЛЕЙ

UDC 532.526.4

THEORY OF TURBULENCE AND SIMULATION OF TURBULENT TRANSPORT IN THE ATMOSPHERE PART 6

Alexander Trunev
Ph.D.
Director, A&E Trounev IT Consulting, Toronto, Canada

The model of continuous transition from the laminar flow to the turbulent flow is proposed and the theory of the spectral density of turbulent pulsation is given

Keywords: ACCELERATED FLOW, AEROSOL TURBULENT TRANSPORT, ATMOSPHERIC STRATIFIED FLOW, ATMOSPHERIC TURBULENCE, ATMOSPHERIC SURFASE LAYER, BOUNDARY LAYER, ROUGH SURFACE, TURBULENT TRANSPORT

6. Dynamics of boundary layer

6.1. Boundary layer structure

During the last twenty years mathematical modeling of turbulent flows of fluid has been successfully developed in several directions at once [1, 19-54, 59-70, 74-128]. Methods of direct numerical simulation (DNS) [66, 116], large eddy simulation (LES) [140], and different models, based on Navier-Stokes equations averaged according to Reynolds's method [28-38, 44, 51] have to do with these directions. The theory of hydrodynamic instabilities and transition to turbulence was proposed, which is based primary on the mathematical ideas about behavior of the dynamical systems [141-142]. The fractal geometry theory developed by Mandelbrot [143] has been used to explain the chaos and intermittence in the hydrodynamic turbulence [144-145]. To obtain the numerical solutions of applied multidimensional problems the effective numerical algorithms have been created [146-147].

The boundary layer is a typical self organized flow formed around any rigid body moving in the viscose fluid at high Reynolds number. To illustrate the common problems of the boundary layer theory let us consider the structure of the boundary layer on the flat plate in adverse pressure gradient - see figure 6.1. This flow includes the laminar boundary layer (*1*), the transition flow (*2*), the turbulent boundary layer (*3*) and the separated turbulent flow (*4*).

The laminar boundary layer is a well predicted and sufficiently investigated flow. But this flow is not a stable at high Reynolds number, because it can be like an amplifier for the waves of small amplitude.

The transition layer has a complex structure considered by many authors [62, 141, 145, 149-151]. As it was shown by Jigulev [149] and Betchov [150] this flow domain includes seven sub-regions:

1) the laminar flow region in which the small disturbances are generated. This part of flow is considered often as a starting point of transition layer. The Reynolds number of initial point of transition layer is a very sensitive to the boundary conditions on the wall and in the outer flow. The estimated value of the Reynolds number of transition is $\mathrm{Re}_{tr} = x_{tr} U_0 / n \approx 4 \cdot 10^5$ and as high as $\mathrm{Re}_{tr} \approx 4 \cdot 10^6$;

2) the quasi-laminar flow region in which the amplitude of linear waves (called the Tollmien-Schlichting waves) grows up to the critical value $dU / U_0 \cong 10^{-2}$. The typical scale of this region is about $\Delta x \approx 10^2 H$, where H is a local thickness of the boundary layer;

3) the nonlinear critical layer where the interaction between waves and main flow leads to the new unstable state. The typical scale of this region can be estimated as $\Delta x \approx 10H$;

4) 3D waves region with scale $\Delta x \approx H$. In this region initial two-dimensional waves are transformed into three-dimensional waves;

5) the region of the secondary instability in which the short length waves are generated. The typical scales of this zone are about $\Delta x \approx 0.1H$, $dU / U_0 \cong 10^{-1}$;

6) the Emmons sports region with typical scales $\Delta x \approx H$, $dU / U_0 \cong 3 \cdot 10^{-1}$. In this part of flow the non-equilibrium process leads to the turbulent spectrum of velocity fluctuations;

7) the initial region of the turbulent flow in which $dU / U_0 \cong 3 \cdot 10^{-2}$.

The transition from the laminar flow to the turbulent flow is a very attractive phenomenon from the mathematical point of view. Really the initial laminar flow, which is not consisting of any chaotic waves, then suddenly transforms to the state with a chaotic behavior. This problem of transformation called "dynamical chaos" has been investigated by many authors (see for instance [142, 145]).

The theory of the "dynamical chaos" is based mostly on the analyses of the simplifier dynamical systems (Lorenz-like chaos) which can't be used directly for the boundary layer problem.

The turbulent boundary layer is characterized by chaotic pulsation of the flow parameters. The surface which separates the turbulent stream from the outer flow looks like a rough surface. The thickness of the turbulent boundary layer in zero pressure gradient increases with a distance approximately as a power function $H / x \approx 0.37 \mathrm{Re}_x^{-0.2}$, and the skin friction coefficient slowly decreases with the

Reynolds number increasing as $c_f \approx 0.059\,\mathrm{Re}_x^{-0.2}$ where $\mathrm{Re}_x = U_0 x / n$ (see Schlichting [61]).

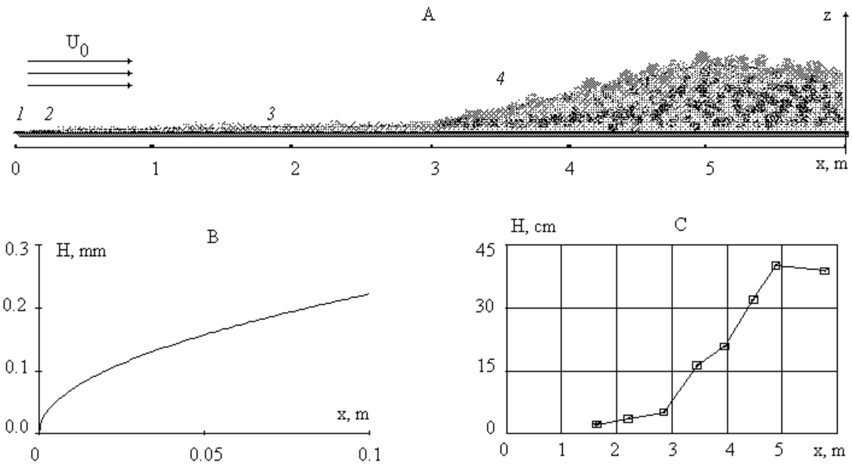

Figure 6.1: A) The boundary layer on the flat plate in adverse pressure gradient: *1* - laminar boundary layer; *2* - transition layer; *3* - turbulent boundary layer; *4* - turbulent separated flow; B) the thickness of the laminar boundary layer in the air flow at $U_0 = 31.47 m/s$; C) the mean height of the separating boundary layer according to Simpson *et al* [148]

The turbulent boundary layer in adverse pressure gradient separates out from the rigid surface and the boundary layer thickness increases as it is shown in Figure 6.1,c. This part of the boundary layer is not so well predictable as a laminar flow, thus till now the separated turbulent boundary layers were studied only in partial cases primary by experimental way (see Simpson *et al* [148]).

The turbulent boundary layer can be modelled on the theory of turbulence which was explained in Chapter 2. But it is a very interesting fact that the laminar flow and transition layer also can be described by the equation system (2.14) derived from the Navier-Stokes equations (NSE) due to the special type of transformation (2.1). Let us consider the application of the turbulence theory to the quasi-laminar boundary layer, i.e. to the boundary layer flow which has some symptoms of turbulent flow.

6.2. Laminar boundary layer

The general solution for the laminar flow can be found on the base of the boundary layer approximation of the Navier-Stokes equations in the Prandtl's form:

$$\begin{aligned} &\frac{\partial u}{\partial x} + \frac{\partial w}{\partial z} = 0 \\ &u\frac{\partial u}{\partial x} + w\frac{\partial u}{\partial z} + \frac{1}{r}\frac{\partial p}{\partial x} = n\frac{\partial^2 u}{\partial z^2} \end{aligned} \tag{6.1}$$

Here the pressure gradient is given by equation (4.17), thus

$$rU_0 \frac{\P U_0}{\P x} = -\frac{\P p}{\P x}. \tag{6.2}$$

To derive model (6.1) from the Navier-Stokes equations we should suppose that

a) the laminar boundary layer is a two-dimensional flow, i.e. $\mathbf{v} = \mathbf{v}(x,z) = (u,0,w)$;

b) the normal to the wall velocity gradient sufficiently exceeds the parallel to the wall velocity gradient, i.e. $|\partial u/\partial z| >> |\partial u/\partial x|$;

c) the normal to the wall pressure gradient is so small that it can be neglected, therefore the pressure distribution is described by the Bernoulli equation (6.2).

It can be shown that the sufficient condition, to satisfy suppositions b)-c), is that the Reynolds number computed on the distance from the plate edge has an extremely high value, i.e. $\mathrm{Re}_x = xU_0/n >> 1$.

Boundary conditions for the quasi-linear diffusion equation (6.1) can be set as follows:

$$\begin{aligned} &x = 0, z \geq 0 : u(0,z) = U_0(0) \\ &x > 0, z = 0 : u(x,0) = w(x,0) = 0 \\ &x > 0, z \to \infty : u(x,z) \to U_0(x) \end{aligned} \tag{6.3}$$

The first equation (6.1) can be satisfied automatically if we define a flow function as follows

$$u = \frac{\partial \hat{y}}{\partial z}, \quad w = -\frac{\partial \hat{y}}{\partial x} \tag{6.4}$$

Problem (6.1)-(6.3) has a self-similarity solution for the boundary layer in a zero pressure gradient. In this case $U_0(x) = U_0(0) = const$, thus the first and third condition (6.3) are identical that means that a solution of this problem depends on the universal variable $h = z/\sqrt{nx/U_0}$. Put $\hat{y} = \sqrt{xnU_0}\, f(h)$, then the velocity components can be rewritten as functions of the universal variable, i.e.,

$$u = \frac{\partial \hat{y}}{\partial z} = U_0 f', \quad w = -\frac{\partial \hat{y}}{\partial x} = \frac{1}{2}\sqrt{\frac{nU_0}{x}}(h\, f' - f) \tag{6.5}$$

Substituting these expressions in the second equation (6.1) one can find that the universal function $f(h)$ is described by the following equation (see, for example, [51, and 58]):

$$2f''' + ff'' = 0 \tag{6.6}$$

The boundary conditions for equation (6.6) (these conditions can be derived from (6.3)) have a form

$$f(0) = f'(0) = 0, \quad f'(\infty) = 1 \tag{6.7}$$

The problem (6.6-6.7) can be solved numerically using the algorithm described above in subsection 2.4.2. For the initial iteration one can put $f''(0) = 0.33206$ (see [51]) that gives in practice the precise solution. Obviously that it's impossible to satisfy last condition (6.7) in a numerical procedure. Hence instead of it as usual the boundary condition in the outer region has used, $f'(h_e) = 0.9999$ where $h_e \approx 8$ [51]. Thus the boundary layer depth can be defined as a point where, for instance, $z_e/\sqrt{nx/U_0} = 8$, i.e.

$$H(x) \propto \sqrt{nx/U_0} \tag{6.8}$$

This function is shown in Figure 6.1,b to illustrate the typical scale of laminar boundary layer in the air flow at $U_0 = 31.47 m/s$. Therefore the universal variable can be presented as $h = z/h(x)$, where $h(x) = \sqrt{nx/U_0}$ is the boundary layer characteristic thickness

The boundary layer thickness is not a constant; it slowly increases down to the stream so that

$$\frac{dh}{dt} = U_0 \frac{dh}{dx} = \frac{1}{2}\sqrt{\frac{nU_0}{x}} \tag{6.9}$$

This equation gives the normal to the wall velocity scale which can be defined as $w_0 = dh/dt$. With two characteristic scales of velocity equations (6.5) can be rewritten as follows:

$$u/U_0 = f', \quad w/w_0 = h\, f' - f \tag{6.10}$$

The normalised velocity profiles in the laminar boundary layer are shown in Figure 6.2. The normal to the wall velocity normalised on the scale $w_0 = dh/dt$ has a limit value at $h \to \infty$: $w/w_0 = 1.72$. The positive value of this velocity component means that the stream lines starting from the boundary layer then penetrate in the outer flow region.

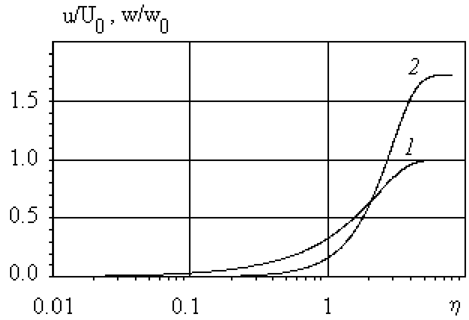

Figure 6.2: The normalised velocity profiles in the laminar boundary layer in zero pressure gradient: *1* - u/U_0; *2* - w/w_0

The normal to the wall velocity scale decreases with distance as $w_0 = 0.5U_0 \, \mathrm{Re}_x^{-0.5}$. Thus near the transition layer this scale has a very small value which has never been taken into account in the theory of transition to turbulence.

The skin friction coefficient can be defined for the laminar flow as $c_f = (n\partial u/\partial z)/(U_0^2/2) = 2f''(0)/\sqrt{\mathrm{Re}_x}$. Substituted in this formula the numerical value of the second derivative, $f''(0) = 0.33206$, which was calculated above, we have $c_f = 0.664/\sqrt{\mathrm{Re}_x}$.

The self-similarity solutions (6.5) found for the laminar flow (called the Blasius flow) is only type of the self-similarity solutions of the Navier-Stokes equations (NSE). Let us give a proof that the Blasius flow can be described by equation system (2.14). Really all solutions of the equation system (2.14) which was derived from NSE are presented by the self-similarity functions. Therefore, we can select from (2.14) also solution for the Blasius flow. First of all note that in this two-dimensional flow $\Psi = h_y u - h_x \mathrm{v} = 0$, and $\Phi = h_x u$, hence we have

$$\frac{\partial \tilde{W}}{\partial h} + h_x u = 0 \qquad (6.11)$$

$$\frac{\tilde{W}}{h}\frac{\partial^2 \tilde{W}}{\partial h^2} = \frac{n}{h^2}\frac{\partial}{\partial h}(1 + n^2 h^2)\frac{\partial^2 \tilde{W}}{\partial h^2},$$

Here $\tilde{W} = w - h_x uh$. Let $\tilde{W} = -U_0 h_x f(h)$, then the generalised form of (6.5) and (6.6) can be found from first eq. (6.11) and from the definition of $\tilde{W}$ immediately as follows

$$u = U_0 f', \quad w = h_x U_0 (h\, f' - f) \tag{6.12}$$

$$f \frac{\partial^2 f}{\partial h^2} + \frac{n}{h h_x U_0} \frac{\partial}{\partial h}(1 + h_x^2 h^2) \frac{\partial^2 f}{\partial h^2} = 0 .$$

The Blasius solution corresponds to the special case when

$$n/(h h_x U_0) = 2\,, \quad h(x) = \sqrt{nx/U_0}\,. \tag{6.13}$$

In this case the second eq. (6.12) has a form

$$f \frac{\partial^2 f}{\partial h^2} + 2 \frac{\partial}{\partial h}(1 + h^2/4\,\mathrm{Re}_x) \frac{\partial^2 f}{\partial h^2} = 0 \tag{6.14}$$

The boundary layer approximation (6.1) is applicable only for very high Reynolds number, i.e. for $\mathrm{Re}_x = xU_0/n >> 1$. Hence the term in the brackets which is proportional to $1/\mathrm{Re}_x$ can be neglected in (6.14) and finally we have equation (6.6).

6.3. Transition to turbulence

6.3.1. Continuous transition to turbulence

Passing through the transition layer the laminar stream transforms into the turbulent flow. There are several models of transition to turbulence (see [58, 141, 145, 149] and other). From the point of view of the turbulence theory considered above the parameter characterized the dynamical roughness structure, i.e. $a = \arctan(h_y/h_x)$, increases in the transition layer from a zero up to $a = p/2$, and the second turbulent velocity scale, $w_0^+ = h_t/u_* \sqrt{h_x^2 + h_y^2}$, increases from a zero up to $w_0^+ \approx 0.14$. Consequently the 2D laminar Blasius flow transforms into 3D turbulent flow.

The general solution (2.16) of the turbulent incompressible flow model (2.14) can be used to analyze the transition from the Blasius flow to the turbulent flow. Put $A_1 = h_x u_h(0),\ A_2 = h_y u_h(0)$ in this solution then the random velocity components can be written as follows

$$\frac{d\tilde{u}}{dh} = u_h(0) e^{-I} \left(\frac{\cos^2 a}{1 + n^2 h^2} + \frac{\sin^2 a}{\sqrt{1 + n^2 h^2}} \right), \tag{6.15}$$

$$\frac{d\,\tilde{\mathrm{v}}}{dh} = \frac{1}{2} u_h(0) e^{-I} \sin 2a \left(\frac{1}{1 + n^2 h^2} - \frac{1}{\sqrt{1 + n^2 h^2}} \right),$$

$$\frac{d\tilde{w}}{dh} = \frac{u_h(0)nhe^{-I}\cos a}{1+n^2h^2}$$

where $I = -\frac{h}{n}\int^h \frac{\tilde{W}dh}{1+n^2h^2}$.

Put $\tilde{W} = -h_x U_0 f(h)$ as in the case of the Blasius flow then we have

$$I = \frac{U_0 hh_x}{n}\int_0^h \frac{f dh}{1+n^2h^2} \tag{6.16}$$

where a function $f = f(h)$ satisfies to equation

$$f\frac{\partial^2 f}{\partial h^2} + \frac{n}{hh_x U_0}\frac{\partial}{\partial h}(1+n^2h^2)\frac{\partial^2 f}{\partial h^2} = 0 \tag{6.17}$$

with boundary conditions

$$f(0) = 0, \quad f'(0) = h_t / U_0 h_x, \quad f''(0) = u_h(0)/U_0 . \tag{6.18}$$

Put $n/(hh_x U_0) = 2$ in (6.17) as for the Blasius flow solution, therefore

$$h(x,y,t) = \sqrt{nx/U_0 + Q(t,y)} , \tag{6.19}$$

where $Q(t,y)$ is an arbitrary function.

6.3.2. 3D Transition to turbulence

The first scenario of spatial continuous transition to turbulence is that $h_t = 0$ and $f''(0) = 0.33206$. In this case the boundary conditions (6.18) are similar to the Blasius flow conditions. For $h_y = 0$ we have exactly the Blasius flow solution - see Figure 6.3. Put $Q << nx/U_0$ then the dynamical roughness parameters are given by

$$n^2 \approx 1/4\,\mathrm{Re}_x + h_y^2, \qquad a = \arctan(2h_y\sqrt{\mathrm{Re}_x}) . \tag{6.20}$$

As it follows from this equations if h_y increases then the dynamical roughness parameters also increase and the laminar boundary layer velocity profile (the Blasius profile (*1*) in Figure 6.3) transforms into the turbulent boundary layer velocity profile (*6*) - see Figure 6.3.

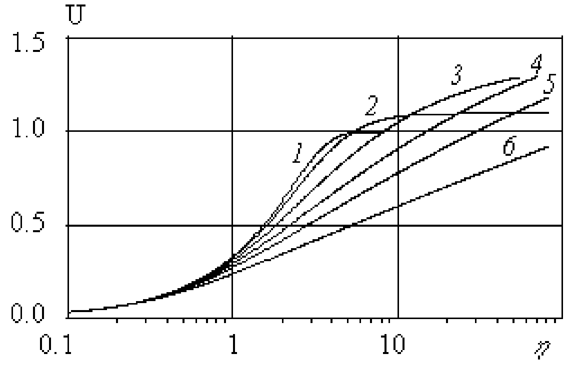

Figure 6.3: Continuous transition from the laminar flow (the Blasius velocity profile (*1*)) to the turbulent flow (the logarithmic velocity profile (*6*)). Profiles *1-6* are computed on (6.17)-(6.18) for $h_t = 0$ and for $h_y = 0; 1/3; 2/3; 1; 4/3; 2$ respectively

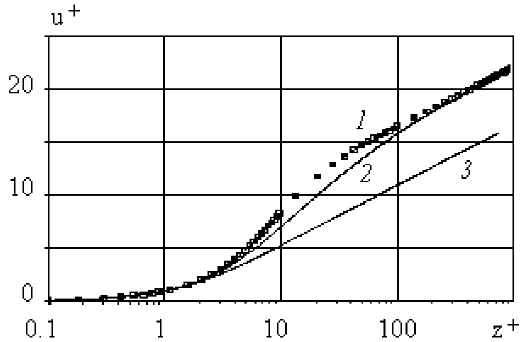

Figure 6.4: Continuos transition to turbulence: *1* - the mean velocity profile in the turbulent boundary layer according to Van Driest [65], *2, 3* - the mean velocity profiles in the transition layer computed on the model (6.24), (6.25) for $h_y = 0.91, 3.5$ respectively

Theoretically the logarithmic profile in this model can be only at $n \to \infty$, but practically the logarithmic asymptotic is realised for $n = 3.5$ - see Figure 6.4. It can be explained by the asymptotic behavior of a solution of equation (6.17) at $h \to \infty$: $f(h) \approx g(n)h - b(n)$, where $b(n), g(n)$ are some parameters. Obviously, that for the Blasius flow $b(0) = w(\infty)/w_0 = 1.72, g(0) = 1$, and in a common case $b(n) \approx 1/2n$ for $n \geq 1$. Therefore $I(h)$ can be estimated for $h \to \infty$ as follows

$$I = \frac{1}{2}\int_0^h \frac{f\,dh}{1 + n^2 h^2} = I_0(n) + \frac{g}{4n^2}\ln(1 + n^2 h^2) \qquad (6.21)$$

$$I_0 = \frac{1}{2}\int_0^\infty \frac{(f - gh)dh}{1 + n^2h^2} .$$

Substituted this expression in the first equation (6.15) and supposed that $a = p/2$ one can derive the asymptotic formula for the streamwise velocity gradient, i.e.

$$\frac{d\tilde{u}}{dh} \approx \frac{u_h(0)e^{-I_0}}{nh}(nh)^{-b},\, nh >> 1 \tag{6.22}$$

Here $b = g/2n^2 \approx 1/4n^3$ for $n \geq 1$. Used the inner layer variables for the mean velocity scaling the last equation can be rewritten as follows

$$\frac{du^+}{dz^+} \approx \frac{l^+e^{-I_0}}{z^+}\left(\frac{l^+}{z^+}\right)^b . \tag{6.23}$$

Calculated the exponent b for $n = 3.5$ we have $b \approx 0.006$. Thus in this case the power function factor in the right part of equation (6.23) is about unit for $10^{-3} \leq z/l \leq 10^3$ hence equation (6.23) leads to the logarithmic profile asymptotic

$$\frac{du^+}{dz^+} \approx \frac{1}{kz^+}$$

Here $k = e^{I_0}/l^+$ is the Karman constant. Using the relationship $l^+ = e^{I_0}/k$ third boundary condition (6.18) in a case of mean velocity profile can be transformed as follows

$$f''(0) = u_h(0)/U_0 = (du^+/dz^+)h^+/U_0^+ = n\,l^+/U_0^+ = ne^{I_0}/kU_0^+$$

Using the inner layer variables we can rewrite the model of spatial transition to turbulence in the form

$$\frac{du^+}{dz^+} = e^{-I}\left(\frac{\cos^2 a}{1 + (z^+/l^+)^2} + \frac{\sin^2 a}{\sqrt{1 + (z^+/l^+)^2}}\right), \tag{6.24}$$

$$Rf\frac{\partial^2 f}{\partial h^2} + \frac{\partial}{\partial h}(1 + n^2h^2)\frac{\partial^2 f}{\partial h^2} = 0\,, \quad I = R\int_0^h \frac{f\,dh}{1 + n^2h^2}\,,$$

$$I_0 = R\int_0^\infty \frac{(f - gh)dh}{1 + n^2h^2}\,,\; g = \lim_{h\to\infty} f(h)/h\,,$$

where $a = \arctan(2h_y\sqrt{\mathrm{Re}_x})$, $n^2 \approx 1/4\mathrm{Re}_x + h_y^2$, $h = z^+/h^+$, $R = hh_xU_0/n = 1/2$ (as for the Blasius flow), $h^+ = n\,l^+$, $l^+ = e^{I_0}/k$. The boundary conditions for this model are given by

$$u^+(0) = 0, \quad f(0) = 0, \quad f'(0) = 0, \quad f''(0) = ne^{I_0}/kU_0^+ \tag{6.25}$$

The mean velocity profiles computed on the model (6.24) for $h_y = 0.91, 3.5$ (the solid lines *2,3*) together with the mean velocity profile in the turbulent boundary layer proposed by Van Driest [65] (the symbolised line *1*) are shown in Figure 6.4. The logarithmic asymptotic of the profile (*3*) has a form $u^+ = k^{-1}\ln z^+ + c_t$, where $c_t = -0.1566$.

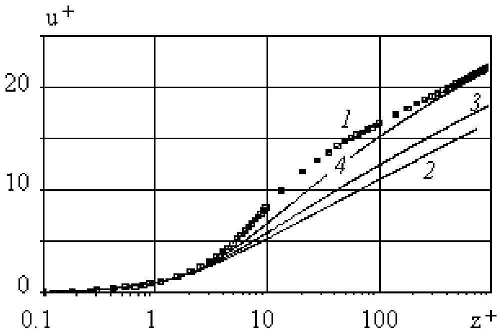

Figure 6.5: Continues transition to turbulence: *1* - the mean velocity profile in the turbulent boundary layer according to Van Driest [65], *2-4* - the mean velocity profiles in the transition layer computed on the model (6.24), (6.26) for $h_y = 3.5$ and $\nu = 0; 1; 2.537$ respectively

The main difficulty of model (6.24) is that the estimated streamwise velocity profile (*3*) is not really the logarithmic profile in the turbulent boundary layer over smooth surface as it should be, but it is the logarithmic profile which can be in the turbulent boundary layer over a rough surface. Thus the skin friction coefficient of this flow is higher then in the turbulent boundary layer with the similar thickness and free stream velocity.

The second scenario of continuous transition to turbulence is that $n \approx 1$ and $h_t / U_0 h_x = \nu$. In this case the transition layer model is identical to (6.24) with boundary conditions

$$u^+(0) = 0, \quad f(0) = 0, \quad f'(0) = \nu, \quad f''(0) = ne^{I_0} / kU_0^+ \qquad (6.26)$$

Using the constant of the logarithmic profile, we can estimate an additional parameter, i.e. ν. The mean velocity profiles computed on the model (6.24), (6,26) for $h_y = 3.5$ and $\nu = 0; 1; 2.537$ are shown in Figure 6.5 - the solid lines (*2-4*) respectively.

This model consists of three parameters n, ν, k while in the turbulent boundary layer there is only one parameter - the Karman constant.

6.3.3. 2D Transition to turbulence

It's a well known fact that the transition layer includes the quasi-laminar flow region in which the amplitude of linear Tollmien-Schlichting waves grows up to the critical value $dU / U_0 \cong 10^{-2}$. This 2D transition zone can be described by the model (6.24) rewritten in the outer region variables. Put in system (6.24) $a = 0, n = 0$. In this case we have 2D transition model

$$Rf\frac{d^2 f}{dh^2} + \frac{d^3 f}{dh^3} = 0, \quad \frac{1}{U_0}\frac{du}{dh} = \frac{c_f \operatorname{Re}_h}{2} e^{-I}, \quad I = R\int_0^h f dh \tag{6.27}$$

with boundary conditions

$$u(0) = 0, \quad f(0) = 0, \quad f'(0) = v, \quad u(\infty) = U_0 \tag{6.28}$$

where $R = hh_x U_0 / n = 1/2$ (as for the Blasius flow), $\operatorname{Re}_h = hU_0 / n$.

This model depends on only free parameter $v = h_t / U_0 h_x$. The streamwise velocity profiles computed on this model for $v = 0; 1; 10$ are shown in Figure 6.6 left, by the solid lines (*1-3*) respectively. This solutions are similar to the Blasius flow solutions for a laminar flow with gas injection (see Cebeci & Bradshaw [51]).

The numerical data for dimensionless velocity gradient, $c_f \operatorname{Re}_h / 2 = u_h(0) / U_0$, are plotted in Figure 6.6 right. These data can be approximated as follows (see the solid line in Figure 6.6 right)

$$c_f \operatorname{Re}_h / 2 = 0.332 + 0.286 v^{0.75} \tag{6.29}$$

where $\operatorname{Re}_h = \sqrt{\operatorname{Re}_x}$ as for the Blasius flow.

There is no a logarithmic profile in 2D flow, but in this type of transition the drag increases up to the value which is typical for the turbulent boundary layers. Really, substituting an expression of the roughness surface parameter $v = h_t / U_0 h_x = 2(h_t / u_*) \operatorname{Re}_h \sqrt{c_f / 2}$ in formula (6.29) we can derive an equation for the skin friction coefficient as follows

$$c_f / 2 = c_f^0 / 2 + 0.286 (2h_t / u_*)^{0.75} (c_f / 2)^{0.375} \operatorname{Re}_x^{-0.125} \tag{6.30}$$

where $c_f^0 = 0.664 / \sqrt{\operatorname{Re}_x}$ is the skin friction coefficient for the Blasius flow.

Supposing in the equation (6.30) that $c_f >> c_f^0$ and expressing the skin friction coefficient in an explicit form, finally we have

$$c_f \approx 0.27 (2h_t / u_*)^{1.2} \operatorname{Re}_x^{-0.2} \tag{6.31}$$

For $h_t / u_* = 0.14$ the last equation exactly gives the Schlichting formula for the skin friction coefficient in the turbulent boundary layer, i.e. $c_f \approx 0.059 \operatorname{Re}_x^{-0.2}$ (see Schlichting [61]). It means that the transition to turbulence is characterized mostly by the parameter $v = h_t / U_0 h_x$ which has a high value $v \approx 10$ in the beginning of the turbulent boundary layer. Hence in this case another scaling should be proposed to balance the dynamical roughness parameters effect on the turbulent flow.

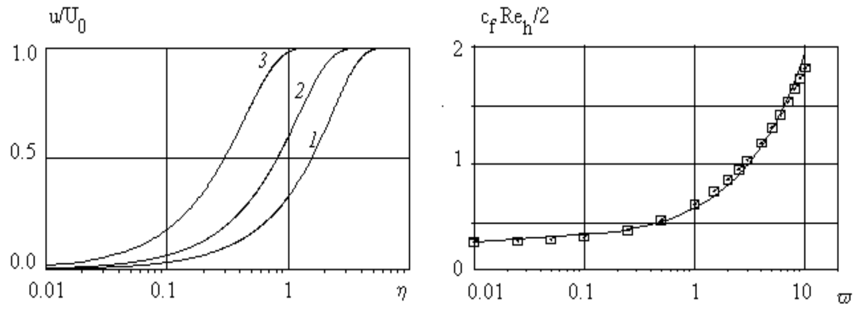

Figure 6.6: The velocity profiles in 2D transition layer calculated on (6.27)-(6.28) for $v = 0; 1; 10$ - the solid lines (*1*-*3*) respectively (left); the normalised skin friction coefficient versus the dynamical roughness surface parameter $v = h_t / U_0 h_x$ (square symbols) together with the approximated solid line (right)

On the other hand as it was shown in subsection 2.4.3, in the turbulent boundary layer also we have $h_t / nu_* = 0.14$. Thus the typical value of the dynamical roughness gradient parameter is about $n \approx 1$. Taken into account that $n^2 \approx 1/4\mathrm{Re}_x + h_y^2 \approx h_y^2$ we can conclude that the transversal gradient $h_y \approx 1$, therefore $a = \arctan(2h_y\sqrt{\mathrm{Re}_x}) \approx p/2$. Obviously that a negative value $h_y \approx -1$ also available with the same probability as a positive value, because as it follows from second equation (6.15) $\tilde{\mathrm{v}} \propto \sin 2a$, and hence the mean transversal velocity $\langle \tilde{\mathrm{v}} \rangle \propto \langle \sin 2a \rangle = 0$.

6.4. Spectral characteristics of turbulent flows

The turbulent boundary layer can also be described by equations system (6.24). Put $a = p/2$ in the first equation (6.24). Substituting an universal variable $x = nh$ and an universal function $c_1 = (n/v)f$ in the second and third equations (6.24) we have

$$\frac{du^+}{dz^+} = \frac{e^{-I}}{\sqrt{1 + (z^+/l^+)^2}} \ , \quad I = R_t \int_0^x \frac{c_1 dx}{1 + x^2}, \qquad (6.32)$$

$$R_t c_1 \frac{\partial^2 c_1}{\partial x^2} + \frac{\partial}{\partial x}(1 + x^2)\frac{\partial^2 c_1}{\partial x^2} = 0,$$

Here $R_t = hh_t / nn^2$ is the Reynolds number calculated on the dynamical roughness parameters. The boundary conditions for this model can be proposed as follows

$$u^+(0) = 0, \quad c_1(0) = 0, \quad c_1'(0) = 1, \quad c_1''(0) = a \tag{6.33}$$

Where a is a free parameter. To establish this parameter it can be claimed that the streamwise mean velocity profile has a logarithmic asymptotic at $z^+ >> l^+$. Surmising that $\lim_{x\to\infty} I(x, R_t) = I_0(R_t)$ we have from the first equation (6.32) $du^+ / dz^+ = l^+ e^{-I_0} / z^+$, and therefore $l^+ = e^{I_0} / k$.

The last equation gives the continuous spectrum of the turbulent scales $l^+ = l^+(R_t)$. On the other hand the mean velocity profile in the logarithmic layer can be characterized by one scale. To solve this problem note, that equation $l^+ = e^{I_0} / k$ can be rewritten in the form

$$w_0^+ = kR_t \exp[-I_0(R_t)], \tag{6.34}$$

Here $w_0^+ = h_t / nu_*$ is the second turbulent velocity scale.

For an uniqueness of the mean velocity profile one can suppose that for $k = const$ the second turbulent velocity scale has a stable value at small variations of the parameter R_t, i.e. $dw_0^+ / dR_t = 0$ (or for $w_0^+ = const$ the Karman constant has a stable value, i.e. $dk / dR_t = 0$). It gives $R_t = R_t^* \approx 1.22$ and $w_0^+ \approx 0.14$ for $k = 0.41$. The fundamental turbulent boundary layer scale can be defined as $l_0^+ = e^{I_0(R_t^*)} / k = 8.71$. The mean velocity profile calculated on this model for $R_t = 1.22$, $l_0^+ = 8.71$ and for $k = 0.41$ is shown in Figure 2.4, a.

The function $1/l^+ = ke^{-I_0}$ can be considered as a spectral density. The inverse length scale versus the Reynolds number is shown in Figure 6.7, a. This type of a spectral density is similar to the spectral density of the streamwise velocity fluctuations in the turbulent boundary layers. The function $w_0^+ = w_0^+(R_t)$ is shown in Figure 6.7, b. This type of spectrum is similar to the spectral density of the transversal velocity pulsation (see Tennekes & Lumley [152]). Both functions represent the constructive model of the hydrodynamic chaos in this theory of turbulence.

To compare the spectral density with experimental data we can suppose that $h_t \propto wh$, where w is the characteristic radian frequency. Therefore the Reynolds number calculated on the dynamical roughness parameters depends on the frequency as

$$R_t = wh^2 / nn^2 = wl_*^{+2} n / u_*^2 = kHl_*^{+2} u^+ / \mathrm{Re}_* \tag{6.35}$$

Here l_*^+ is the typical turbulent length scale of the streamwise velocity pulsation, $k = w/U$ is the flow wave number (Taylor's frozen turbulence hypothesis), $\mathrm{Re}_* = Hu_*/n$. The equation (6.35) can be proved easily, because the non-linear part of the model (6.32) depends on the random parameter R_t only, and it's independent of time. The spectral density of the streamwise velocity pulsation can be defined as follows

$$\int F(k)dk = \int u'^2(w)dw = \lim_{T\to\infty}\frac{1}{T}\int_0^T u'^2(t)dt = \left\langle u'^2\right\rangle \tag{6.36}$$

There are several models which have been proposed to describe the spectral density in the turbulent boundary layers (see Simpson *et al* [148], Tennekes & Lumley [152], Perry *et al* [154] and other). The widely used spectral density in the logarithmic layer is given by $F(k) \approx u_*^2 k^{-1}$. Instead of this we suggest that the spectral characteristic of the turbulent flow is related to the eigen spectrum of the problem (6.32)-(6.33), thus

$$F(k) = c_K \frac{Hu_*^2}{l^+} = kc_K Hu_*^2 e^{-I_0[R_t(k)]} \tag{6.37}$$

Here c_K is the normalizing factor which can be calculated from (6.36).

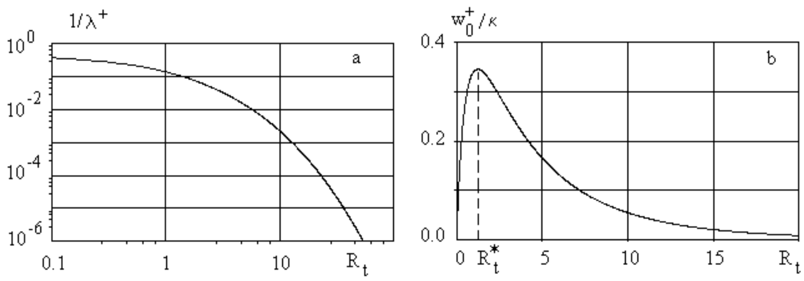

Figure 6.7: The inverse length scale $1/l^+$(a) and the normalised velocity scale w_0^+/k (b) versus the Reynolds number calculated on the dynamical roughness parameter

Suggesting that the flow wave number in the logarithmic layer depends on the dynamical roughness Reynolds number as the linear function, i.e. $k \propto R_t$, we have

$$\left\langle u'^2\right\rangle = \int F(k)dk = \frac{c_K u_*^2\,\mathrm{Re}_*}{u^+ l_*^2}\int\frac{dR_t}{l^+} \approx 0.47\frac{c_K u_*^2\,\mathrm{Re}_*}{u^+ l_*^2}, \tag{6.38}$$

therefore $c_K = 2.13\, l_*^2 u^+ \left\langle u'^2\right\rangle / u_*^2\,\mathrm{Re}_*$.

The spectral density computed on (6.35), (6.37) is shown in Figure 6.8 (solid lines) together with the experimental data by Hussain & Reynolds [153] obtained in the turbulent channel flow. The experimental values and estimated parameters for the data are listed in Table 6.1. The boundary layer height $H = 3.175\,cm$, the mean velocity on the channel axis $U_0 = 13.8\,m/s$, the Reynolds number of the turbulent boundary layer $\mathrm{Re} = HU_0/n = 28600$, and $\mathrm{Re}_* = 1220$.

As it was established both spectral density parameters c_K and l_*^+ slowly depend on the distance from the wall. In the inner layer the experimental data is in a good agreement with the predicted spectral density (a, b). But in the outer region the correlation is not so good (c, d). It can be explained by the mixed layer contribution in the velocity pulsation.

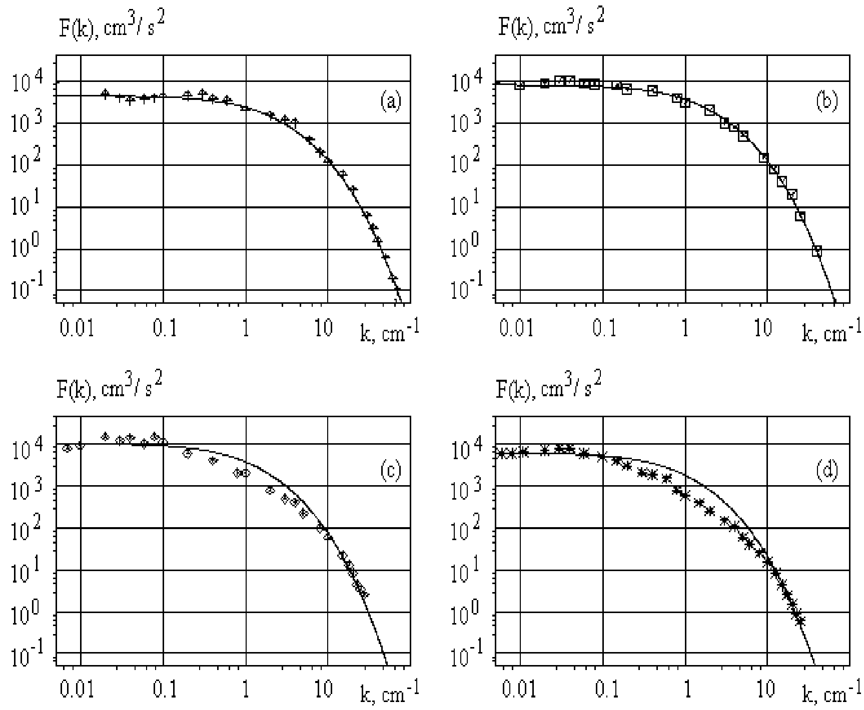

Figure 6.8: The spectral density of the streamwise velocity pulsation in the turbulent channel flow computed on (6.37) (solid lines) and the experimental data by Hussain & Reynolds [153] measured at the distance from the wall $z^+ = 4.9$ (a), $z^+ = 11.7$ (b), $z^+ = 106$ (c), and $z^+ = 770$

Table 6.1 Input data for Figure 6.8

Figure	6.8 a	6.8 b	6.8 c	6.8 d
z^+	4.9	11.7	106	770
l_*^+	6.76	5.45	4.61	4.61
c_K	1.01	1.82	2.27	1.36

The local rate of dissipation of the mean flow kinetic energy in the logarithmic layer is given by

$$\& = -\frac{n}{2}\left(\frac{\partial u}{\partial z}\right)^2 = -\frac{nu_*^2}{2k^2 z^2}$$

The optimal parameter R_t^* brings a maximum for the second turbulent velocity scale and a minimum for the Karman constant. In turn the minimum of the Karman constant is related to the maximum of the local rate of dissipation of the mean flow kinetic energy.

Using the dynamic roughness parameter we can propose the scaling for the local rate of dissipation of the mean flow kinetic energy in the logarithmic layer as follows

$$\& = -2(w_0^* l_0 / z)^2 / t \ ,$$

Here $t = n / u_*^2$ is the scale of time in the inner layer.

Apparently it means that the Karman constant should be determined as $k = 1/2R_t^* \approx 0.41$. Therefore two another constants of the theory are given by $l_0^+ = 2R_t^* e^{I_0(R_t^*)} = 8.71$, $w_0^+ = e^{-I_0(R_t^*)}/2 = 0.14$. This is the final closure. Hence this theory of turbulence is the completely closed theory, because all parameters have been calculated within the theory from the "first principles".

References

[1] Liepmann, H.W., The Rise and Fall of Ideas in Turbulence, *American Scientist*, **67**, pp. 221-228, 1979.

[2] Amirkhanov, M.M, Lukashina, N.S. & Trunev, A. P., *Natural recreation resources, state of environment and economical and legal status of coastal resorts*, Publishing House "Economics", Moscow, 207 p., 1997 (in Russian).

[3] Marchuk, G. I., *Mathematical Modelling in the Environmental Problem*, "Nauka", Moscow, 1982 (in Russian).

[4] Borrell P.M., Borrell P., Cvitas T. & Seiler W., Transport and transformation of pollutants in the troposphere. *Proc. EUROTRAC Symp.*, SPB Academic Publishing, Hague, 1994.

[5] Jaecker-Voirol A., Lipphardt M., Martin B., Quandalle, Ph., Salles, J., Carissimo, B., Dupont, E., Musson-Genon, L., Riboud, P.M., Aumont, B., Bergametti, G., Bey, I., Toupance, G., A 3D regional scale photochemical air quality model - application to a 3 day summertime episode over Paris*, Air Pollution IV. Monitoring, Simulation and Control,* eds. B. Caussade, H. Power & C.A. Brebbia, Comp. Mech. Pub., Southampton, pp. 175-194, 1996.

[6] Borrego, C., Coutinho, M., Carvalho, A.C.& Lemos, S., A modelling package for air quality management in Lisbon, *Air Pollution V. Modelling, Monitoring and Management,* eds. H. Power, T. Tirabassi & C.A. Brebbia, CMP, Southampton-Boston, pp. 35-44, 1997.

[7] Bozo, L.& Baranka, G., Air quality modelling over Budapest, *Air Pollution IV. Monitoring, Simulation and Control,* eds. B. Caussade, H. Power & C.A. Brebbia, Comp. Mech. Pub., Southampton, pp. 31-36, 1996.

[8] Marchuk, G.I. & Aloyan, A.E., Global Admixture Transport in the Atmosphere, *Proc. Rus. Acad. Sci., Phys. Atmosphere and Ocean*, **31**, pp. 597-606, 1995.

[9] Moussiopoulos N., Air pollution models as tools to integrate scientific results in environmental policy, *Air Pollution III, Vol.1. Theory and Simulation,* eds. H. Power, N. Moussiopoulos & C.A. Brebbia, Comp. Mech. Publ., Southampton, pp.11-18, 1995.

[10] Pekar M., *Regional models LPMOD and ASIMD. Algorithms, parametrization and results of application to Pb and Cd in Europe scale for 1990*, EMEP/MSC-E Report 9/96, Aug, 78 p., 1996.

[11] Carruthers, D.J, Edmunds, H.A., McHugh, C.A., Riches, P.J. & Singles, R.J., ADMS Urban - an integrated air quality modelling system for local government, *Air Pollution V. Modelling, Monitoring and Management,* eds. H. Power, T. Tirabassi & C.A. Brebbia, CMP, Southampton-Boston, pp. 45-58, 1997.

[12] Ni Riain, C., Fisher, B., Martin, C. J. & Littler J., Flow field and Pollution Dispersion in a Central London Street, *Proc. of the 1st Int. Conf. on Urban Air Quality: Monitoring and Modelling,* ed. R. S. Sokhi, Kluwer Academic Publishers, pp. 299-314, 1998.

[13] Lukashina, N.S. & Trunev, A. P., *Principles of Recreation Ecology and Natural Economics,* Russian Academy of Sciences, Sochi, 273 p., 1999 (in Russian).

[14] Lukashina, N.S., Amirkhanov, M.M, Anisimov, V.I. & Trunev, A.P., Tourism and environmental degradation in Sochi, Russia, *Annals of Tourism Research*, **23,** pp. 654-665, 1996.

[15] Lenhart, L. & Friedrich, R. European emission data with high temporal and spatial resolution, *Air Pollution III Vol.2: Air Pollution Engineering and management,* eds. H. Power, N. Moussiopoulos & C.A. Brebbia. Comp. Mech. Pub., Southampton, pp.285-292, 1995.

[16] Oke, T.R., Street design and urban canopy layer climate, *Energy and Buildings,* **11,** pp. 103-111, 1988.

[17] Zilitinkevich, S. Non-local turbulent transport: pollution dispersion aspects of coherent structure of convective flows, Air Pollution III, Vol.1. Air Pollution Theory and Simulation, eds. H. Power, N. Moussiopoulos & C.A.Brebbia, Comp. Mech. Publ., Southampton, pp.-53-60, 1995.

[18] Arya, S. P., *Introduction to Micrometeorology,* Academic Press, San Diego, 307 p., 1988.

[19] Stull, R. B, *An Introduction to Boundary Layer Meteorology*, Kluwer Academic Publishers, Dordrecht, 666 p., 1988.

[20] Kaimal, J. C.& Finnigan, J. J., *Atmospheric Boundary Layer Flows: Their Structure and Measurements,* Oxford University Press, 289 p., 1994.

[21] Monin, A.S. & Obukhov, A.M., Basic Laws of Turbulent Mixing in the Atmospheric surface layer, *Trudy Geofiz. Inst. Akad. Nauk SSSR* **24** (151), pp. 163-187, 1954.

[22] Monin, A. S., The Atmospheric Boundary Layer, *Ann. Rev. Fluid Mech.*, **22**, 1970.

[23] Businger, J.A., Wyangaard, J.C., Izumi, Y. & Bradley, E.F. Flux Profile Relationships in the Atmospheric Surface Layer, *J. Atmos. Sciences*, **28.** pp.181-189, 1971.

[24] Businger, J. A., A Note on the Businger-Dyer Profile, *Boundary-Layer Meteorol.*, **42,** pp. 145–151, 1988.

[25] Yaglom, A.M., Data on Turbulence Characteristics in the Atmospheric Surface Layer, *Izv. Acad. Sci. USSR, Phys. Atmosphere and Ocean,* **10**, pp. 566-586, 1974.

[26] Dyer, A. J., A Review of Flux-Profile Relationships, *Boundary-Layer Meteorol.*, **7,** pp. 363–372, 1974.
[27] Van Ulden, A. & Holtslag, A. A. M., Estimation of Atmospheric Boundary Layer Parameters for Diffusion Applications, *J. Clim. Appl. Meteorol,*. **24,** pp. 1196–1207, 1985.
[28] Hanjalic, K.& Launder, B. E., A Reynolds Stress Model of Turbulence and its Application to Thin Shear Flows, *J. Fluid Mech*, **52,** pp. 609–638, 1972.
[29] Rodi, W. Calculation of Stably Stratified Shear-layer Flows with a Buoyancy-extended $k-e$ Turbulence Model, *Turbulence and Diffusion in Stable Environments*, ed. J. C. R. Hunt, Clarendon Press, Oxford, pp. 111–143, 1985.
[30] Mellor, G. L. & Yamada, T. A, Hierarchy of Turbulence Closure Models for Planetary Boundary Layers, *J. Atmos. Sci*., **31,** pp. 1792–1806, 1974.
[31] Mellor, G. L. & Yamada, T., Development of a Turbulence Closure Model for Geophysical Fluid Problems, *Rev. Geophys. Space Phys*., **20,** pp.851–875, 1982.
[32] Wyngaard, J. C. & Cote, O. R., The Evolution of a Convective Planetary Boundary Layer –a Higher-order-closure Model Study, *Boundary-Layer Meteorol.*, **7,** pp. 289–308, 1974.
[33] Zeman, O. & Lumley, J. L., Modelling Buoyancy Driven Mixed Layers, *J. Atmos. Sci*., **33,** pp.1974–1988, 1976.
[34] Deardorff, J. W. & Willis, G. E., Further Results from a Laboratory Model of the Convective Boundary Layer, *Boundary-Layer Meteorol*, **32,** pp. 205–236, 1985.
[35] Enger, L., A Higher Order Closure Model Applied to Dispersion in a Convective PBL, *Atmos. Environ*., **20,** pp. 879–894, 1986.
[36] Holt, T. & Raman, S., A Review and Comparative Evaluation of Multilevel Boundary Layer Parameterisations for First Order and Turbulent Kinetic Energy Closure Schemes, *Rev. Geophys. Space Phys*., **26,** pp. 761–780, 1988.
[37] Danilov, S.D., Koprov, B. M. & Sazonov, L. A., Atmospheric Boundary Layer and the Problem of Its Description (Review), *Proc. Rus. Acad. Sci., Phys. Atmosphere and Ocean*, **31**, pp. 187-204, 1995.
[38] Hurley, P. J., An Evaluation of Several Turbulence Schemes for the Prediction of Mean and Turbulent Fields in Complex Terrain, *Boundary-Layer Meteorol*., **83,** pp. 43–73, 1997.
[39] Reynolds, O., On the dynamically theory of incompressible viscous fluids and the determination of the criterion, *Philos. Trans. R. Soc. London*, **A 186,** 123, 1895.
[40] Boussinesq, J., Theorie de l'ecoulement tourbillat, *Mem. Pres. Acad. Sci.*, **23**, p. 46, 1877.
[41] Prandtl, L., Bericht uber untersuchungen zur ausgebildeten turbulenz, *Z. Angew. Math. Mech*., **5**, pp.136-139, 1925.
[42] Prandtl, L., Neuere Ergebnisse der Turbulenzforschung, VDI -Ztschr., **77,** 5, p.105, 1933.
[43] Kolmogorov, A.N., The Equations of Turbulent Motion in an Incompressible Fluid, *Izv. Acad. Sci. USSR, Phys*., **6,** pp. 56-58, 1942.
[44] Apsley, D. D. & Castro, I. P., A Limited-Length-Scale-Model for the Neutral and Stable-Stratified Atmospheric Boundary Layer, *Boundary Layer Meteorol*., **83,** pp. 75–98, 1997.
[45] Trunev, A. P., Diffuse processed in turbulent boundary layer over rough surface, *Air Pollution III, Vol.1. Theory and Simulation,* eds. H. Power, N. Moussiopoulos & C.A. Brebbia, Comp. Mech. Publ., Southampton, pp. 69-76, 1995.
[46] Trunev, A. P., Similarity theory and model of turbulent dusty gas flow over large-scale roughness, *Abstr. of Int. Conf. On Urban Air Quality: Monitoring and Modelling*, University of Hertfordshire, Institute of Physics, London, p. 3.8, 1996.
[47] Trunev, A. P., Similarity theory for turbulent flow over natural rough surface in pressure and temperature gradients, *Air Pollution IV. Monitoring, Simulation and Control,* eds. B. Caussade, H. Power & C.A. Brebbia, Comp. Mech. Pub., Southampton, pp. 275-286, 1996.
[48] Trunev, A. P., Similarity theory and model of diffusion in turbulent atmosphere at large scales, *Air Pollution V. Modelling, Monitoring and Management,* eds. H. Power, T. Tirabassi & C.A. Brebbia, CMP, Southampton-Boston, pp. 109-118, 1997.
[49] Klebanoff, P. S., Characteristics of turbulence in a boundary layer with zero pressure gradient, *NACA Tech. Note*, **3178**, 1954.
[50] Laufer, J., The structure of turbulence in fully developed pipe flow, *NACA Tech. Note*, **2954**, 1954.

[51] Cebeci, T. & Bradshaw, P., *Physical and Computational Aspects of Convective Heat Transfer*, Springer-Verlag, NY, 1984.
[52] Cantwell, Brian J., Organized motion in turbulent flow, *Ann. Rev. Fluid Mech.*, **13**, pp. 457-515, 1981.
[53] Kuroda, A., *Direct Numerical Simulation of Couette-Poiseuille Flows*, Dr. Eng. Thesis, the University of Tokyo, Tokyo, 1990.
[54] Coleman, G.N., Ferziger, J. R. & Spalart, P. R., A numerical study of the turbulent Ekman layer, *J. Fluid Mech*., **213**. pp.313-348, 1990.
[55] Trunev, A. P. & Fomin, V. M., Continual model of impingement erosion, *J. Applied Mech. Tech. Phys*., **6**, pp. 113-120, 1985.
[56] Trunev, A. P., *Research of bodies erosion distraction in gas flows with admixture particles*, Ph.D. Thesis, Inst. Theoretical and Appl. Mech., Novosibirsk, 1986.
[57] Nikolaevskii, V.N., The space averaging in the turbulence theory, *Vortexes and Waves*, ed. V.N. Nikolaevskii, Mir, Moscow, pp. 266-335, 1984 (in Russian).
[58] Landau, L.D. & Lifshitz, E. M., *Hydrodynamics*, 3rd ed., Nauka, Moscow, 1986 (in Russian).
[59] Pulliam, T. H. & Steger, J. L., Implicit Finite-Difference Simulations of three-dimensional Compressible Flow, *AIAA Journal*, **18,** p. 159, 1980.
[60] Hirschel, E.H. & Kordulla, W., *Shear Flow in Surface-Oriented Coordinates*, Friedr. Vieweg & Sohn, Wiesbaden, 1986.
[61] Schlichting, H., *Boundary Layer Theory*, McGraw-Hill, NY, 1960.
[62] Kutateladze, S.S., *The Wall Turbulence*, Nauka, Novosibirsk, 1973 (in Russian).
[63] Hairer, E., Norsett, S.P. & Wanner, G., *Solving Ordinary Differential Equations 1. Nonstiff Problems*, Springer-Verlag, Berlin, 1987.
[64] Cantwell, B. J., Coles, D. E. & Dimotakis, P. E., Structure and entrainment in the plane of symmetry of a turbulent spot, *J. Fluid Mech.*, **87**, pp. 641-672, 1978.
[65] Van Driest, E.R., On turbulent flow near a wall, *J. Aero. Sci*., **23.** p.1007, 1956.
[66] Kuroda, A., Kasagi, N. & Hirata, M., A Direct Numerical Simulation of the Fully Developed Turbulent Channel Flow, *Proc. Int. Symp. on Computational Fluid Dynamics*, Nagoya, pp. 1174-1179, 1989.
[67] Nagano, Y., Tagawa, M. & Tsuji, T., Effects of Adverse Pressure Gradients on Mean Flows and Turbulence Statistics in a Boundary Layer, *Proc. 8th Symposium on Turbulent Shear Flows*, 1992.
[68] Nagano, Y., Kasagi, N., Ota, T., Fujita, H., Yoshida, H. & Kumada, M., *Data-Base on Turbulent Heat Transfer*, Department of Mechanical Engineering, Nagoya Institute of Technology, Nagoya, DATA No. FW BL004, 1992.
[69] Smith, R.W., *Effect of Reynolds Number on the Structure of Turbulent Boundary Layers*, Ph.D. Thesis, Princeton University, Princeton, NJ, 1994.
[70] Kline, S.J , Reynolds, W.C., Schraub, F.A. & Runstadler P.W., The structure of turbulent boundary layers, *J. Fluid Mech.*, **30**, pp. 741-773, 1967.
[71] Kriklivy, V.V., Trunev, A.P. & Fomin, V.M., Investigation of two-phase flow in channel with damaging wall, *J. Applied Mech. Tech. Phys*., **1**, pp. 82-87, 1985.
[72] Trunev, A. P. & Fomin, V.M., Surface instability during erosion in the gas-particles stream, *J. Applied Mech. Tech. Phys*., **3**. pp. 78-84, 1986.
[73] Trunev, A. P., Evolution of the surface relief at sputtering by ionic bombardment, *Interaction of nuclear particles with a rigid body*, Moscow, Vol.1, Part 1, pp. 83-85, 1989.
[74] Blackwelder, R. F. & Eckelmann, H., Streamwise vortices associated with the bursting phenomena, *J. Fluid Mech.*, **94**, pp. 577-594, 1979.
[75] Nikuradse, J., Strömungsgesetze in Rauhen Rohren, *ForschHft. Ver. Dt. Ing*., p. 361, 1933.
[76] Schlichting, H., Experimentelle Untersuchungen zum Rauhigkeits-problem, *Ing.-Arch*, **7**(1), pp.1-34, 1936.
[77] Bettermann, D., Contribution a l’Etude de la Convection Force Turbulente le Long de Plaques Regueuses, *Int. J. Heat and Mass Transfer*, **9,** p. 153, 1966.
[78] Millionschikov, M.D., *Turbulent flows in the boundary layer and in the tubes*, Nauka, Moscow, 1969 (in Russian).

[79] Dvorak, F. A., Calculation of Turbulent Boundary Layer on Rough Surface in Pressure Gradient, *AIAA Journal*, **7,** 1969.

[80] Dirling, R.B., Jr., A Method for Computing Roughwall Heat-Transfer Rate on Re-Entry Nose Tips, *AIAA Paper*, **73-763**, 1973.

[81] Simpson, R. L., A Generalized Correlation of Roughness Density Effect on the Turbulent Boundary Layer, *AIAA Journal*, **11**, pp. 242-244, 1973.

[82] Donne, M. & Meyer, L., Turbulent Convective Heat Transfer from Rough Surfaces with Two-Dimensional Rectangular Ribs, *Int. J. Heat Mass Transfer*, **20,** pp. 583-620 , 1977.

[83] Coleman, H. W., Hodge, B. K. & Taylor, R. P., A Revaluation of Schlichting's Surface Roughness Experiment, *J. Fluid Eng.*, **106,** pp. 60-65, 1984.

[84] Clauser, F., The Turbulent Boundary Layer, *Advances in Applied Mechanics*, **4,** pp.1-51, 1956

[85] Grabov, R. M. & White, C. O., Surface Roughness Effects on Nose Tip Ablation Characteristics, *AIAA Journal*, **13,** pp. 605-609, 1975.

[86] Sigal, A. & Danberg, J. E., New Correlation of Roughness Density Effect on the Turbulent Boundary Layer, *AIAA Journal*, **25**, pp.554-556, 1990.

[87] Kind, R. J. & Lawrysyn, M. A., Aerodynamic Characteristics of Hoar Frost Roughness, *AIAA Journal*, **30**, pp. 1703-7, 1992.

[88] Gargaud, I. & Paumard, G., *Amelioration du transfer de chaleur par l'emploi de surfaces corruguees*, CEA-R-2464, 1964.

[89] Draycott, A. & Lawther, K.R., Improvement of fuel element heat transfer by use of roughened surface and the application to a 7-rod cluster, *Int. Dev. Heat Transfer*, Part III, pp. 543-52, ASME, NY. 1961.

[90] Möbius, H., Experimentelle Untersuchung des Widerstandes und der Gschwindig-keitsverteilung in Rohren mit regelmäßig angeordneten Rauhigkeiten bei turbulenter Strömung, *Phys. Z.*, **41**, pp. 202-225, 1940

[91] Chu, H. & Streeter, V.L., *Fluid flow and heat transfer in artificially roughened pipes*, Illinois Inst. of Tech. Proc., No. 4918, 1949.

[92] Koch, R., Druckverlust und Wärmeübergang bei verwirbelter Strömung, *ForschHft. Ver. Dt. Ing.*, Series B, **24**, pp. 1-44, 1958.

[93] Skupinski, E., *Wärmeübergang und Druckverlust bei künstlicher Verwirbelung und künstlicher Wandrauhigkeiten*, Diss. Techn. Hochschule, Aachen, 1961.

[94] Webb, R. L., Eckert, E.R.G. & Goldstein, R. J., Heat transfer and friction in tubes with repeated-rib roughness, *Int. J. Heat Mass Transfer*, **14**, pp. 601-617, 1971.

[95] Fuerstein, G. & Rampf, G., Der Einfluß rechteckiger Rauhigkeiten auf den Wärmeübergang und den Druckabfall in turbulenter Ringspaltströmung, *Wärme- und Stoffübertragung*, **2** (1), pp.19-30, 1969.

[96] Sams, E.W., *Experimental investigation of average heat transfer and friction coefficients for air flowing in circular tubes having square-thread-type roughness*, NACA RME 52 D 17, 1952.

[97] Fedynskii, O. S., Intensification of heat transfer to water in annular channel, *Problemi Energetiki*, *Energ. Inst. Akad. Nauk USSR*, 1959 (in Russian).

[98] Watson, M.A.P., *The performance of a square rib type of heat transfer surface*, CEGB RD/B/N 1738, Berkeley Nuclear Laboratories, 1970.

[99] Kjellström, B. & Larsson, A. E., *Improvement of reactor fuel element heat transfer by surface roughness*, AE-271, 1967, Data repoted by Dalle Donne & Meyer (1977).

[100] Savage, D.W. & Myers, J.E., The effect of artificial surface roughness on heat and momentum transfer, *A.I.Ch.E.J.*, **9**, pp.694-702, 1963.

[101] Sheriff, N., Gumley, P. & France, J., *Heat transfer characteristics of roughened surfaces*, UKAEA, TRG Report 447 (R), 1963.

[102] Massey, F.A., *Heat transfer and flow in annuli having artificially roughened inner surfaces*, Ph. D. Thesis, University of Wisconsin, 1966.

[103] Nunner, W., Wärmeübergang und Druckabfall in rauhen Rohren, *ForschHft. Ver. Dt. Ing.*, p. 455, 1956.

[104] Lawn, C. J. & Hamlin, M. J., *Velocity measurements in roughened annuli*, CEGB RD/B/N 2404, Berkley Nuclear Laboratories, 1969

[105] Stephens, M. J., *Investigations of flow in a concentric annulus with smooth outer wall and rough inner wall,* CEGB RD/B/N 1535, Berkley Nuclear Laboratories, 1970.
[106] Perry, A.E. & Joubert, P.N., Rough-Wall Boundary Layers in Adverse Pressure Gradients, *J. Fluid Mech.*, **17**, pp.193-211, 1963.
[107] Antonia, R.A. & Luxton, R.E., The Response of a Turbulent Boundary Layer to a Step Change in Surface Roughness, Pt. 1. Smooth to Rough, *J. Fluid Mech.*, **48**, pp. 721-762. 1971
[108] Antonia, R.A. & Wood, D.H., Calculation of a Turbulent Boundary layer Downstream of a Step Change in Surface Roughness, *Aeronautical Quarterly*, **26**, pp. 202-210, 1975.
[109] Pineau, F., Nguyen, V. D., Dickinson, J. & Belanger, J., Study of a Flow Over a Rough Surface with Passive Boundary-Layer Manipulators an Direct Wall Drag Measurements, *AIAA Paper*, **87-0357,** 1987.
[110] Osaka, H. & Mochizuki, S., Mean Flow Properties of a d-type Rough Wall Boundary Layer in a Transitionally Rough and a Fully Rough Regime, *Trans. JSME ser. B,* .**55**, pp. 640-647, 1989.
[111] Byzova, N.L., Ivanov, V.N. & Garger, E.K., *Turbulence in the Atmospheric Boundary Layer*, Leningrad, Hydrometeoizdat, 1989 (in Russian).
[112] Jackson, P.S., On the displacement height in the logarithmic wind profile. *J. Fluid Mech.*, **111**, pp. 15-25, 1981.
[113] Wieringa, J., Updating the Davenport Roughness Clarification. J. Wind Engineer, *Industl. Aerodyn*, **41**, pp. 357–368, 1992.
[114] Bottema, M., Parameterization of aerodynamic roughness parameters in relation with air pollutant removal efficiency of streets, *Air Pollution III, Vol.2. Air Pollution Engineering and Management*, eds. H. Power, N. Moussiopoulos & C. A. Brebbia, Comp. Mech. Publ., Southampton, pp. 235-242, 1995.
[115] Kutateladze, S. S., *Similarity Analysis in the Thermal-physics*, Novosibirsk, Nauka, 1982 (in Russian).
[116] Kim, J., Investigation of Heat and Mass Transport in Turbulent Flows via Numerical Simulation, *Transport Phenomena in Turbulent Flows: Theory, Experiment and Numerical Simulation*, eds. M. Hirata & N. Kasagi, Hemisphere Publishing Corp., Washington, D. C., pp. 157-170, 1988.
[117] Hogstrom, U., Review of Some Basic Characteristics of the Atmosphere Surface Layer, *Boundary-Layer Meteorol.,* **78**, pp. 215–246, 1996.
[118] Beljaars, A. C. M. & Holtslag, A. A. M., Flux Parameterization over Land Surfaces for Atmospheric Models’, *J. Appl. Meteorol.,* **30**, pp. 327–341, 1991.
[119] Pugliese, S., Jaeger, M. & Occelli, R., Finite element modelling of plume dispersion in the lower part of the atmosphere, *Air Pollution IV. Monitoring, Simulation and Control*, eds. B. Caussade, H. Power & C.A. Brebbia, Comp. Mech. Pub. Southampton-Boston, 99-108. 1996
[120] Lui, Jingmiao & Kotoda, Kazuo, Evaluation of Surface-Layer Wind Profiles With Heife Observations, *Boundary-Layer Meteorol.,* **83,** pp. 27–41, 1997.
[121] Castillo, L., *Similarity analysis of turbulent boundary layers*, Ph. D. Thesis, The Graduate School of the State University of New York, Buffalo, 1997.
[122] Clauser, F.H., Turbulent boundary layer in adverse pressure gradients, *J. Aeron. Sci.*, **21**, pp. 91-108, 1954.
[123] Herring, H. & Norbury, J., Some experiments on equilibrium turbulent boundary layers in favourable pressure gradients, *J. Fluid mech.*, **27**, pp. 541-549, 1967.
[124] Patel, V.C. & Head, M.R., Reversion of Turbulent to Laminar Flow, *J. Fluid. Mech.*, **34,** pp. 371-392, 1968.
[125] Detering, H. W. & Etling, D., Application of the E-e Turbulence Model to the Atmospheric Boundary Layer, *Boundary-Layer Meteorol,* **33,** pp. 113–133, 1985.
[126] Rodi W. Examples of calculation methods for flow and mixing in stratified fluids // *Journal of Geophysical Research*. - 92. - No C5. - 1987. - P. 5305-5328.
[127] Rodi, W., Examples of Turbulence Models for Incompressible Flows, *AIAA Journal*, **20**, pp. 872-879, 1982.
[128] Hassan, A. A. & Crowther, J. M., Modelling of fluid flow and pollutant dispersion in a street canyon, *Proc. of the 1st Int. Conf. on Urban Air Quality: Monitoring and Modelling*, ed. R. S. Sokhi, Kluwer Academic Publishers, pp. 281-297, 1998.

[129] Labatut, A., Cieslik, S., Lamaud, E., Fontan, J. & Druilhet, A., Parameterization of ozone and aerosol particle fluxes, *Air Pollution III, Vol.2. Air Pollution Engineering and Management*, eds. H. Power, N. Moussiopoulos & C. A. Brebbia, Comp. Mech. Publ., Southampton, pp. 141-149, 1995.

[130] Paltridge, G.W. & Platt, C.M.R., *Radiative processes in meteorology and climatology*, Elsevier Scientific Publication Company, Amsterdam, Oxford, New York, 1976.

[131] Jenkins, N., Legassick, W., Sadler, L. & Sokhi, R.S., Correlation between NO and NO_2 roadside concentrations, traffic volumes and local meteorology in major London route, *Air Pollution III, Vol.2. Air Pollution Engineering and Management*, eds. H. Power, N. Moussiopoulos & C. A. Brebbia, Comp. Mech. Publ., Southampton, pp. 405-412, 1995.

[132] Amirkhanov, M.M, Anisimov, V.I., Lukashina, N.S. & Trunev, A. P., Ecological problems of the territorial-recreation complex development of Sochi town, *Izv. Rus. Acad. Sci., Geography*, **1**, pp. 61-71, 1996.

[133] Francois, Ramade, *Elements d'ecologie appliquee*, Group McGraw-Hill, 1978.

[134] Watson A.F.R., Barker S., Ardern K.D. An initial investigation into the potential link between air pollution and asthma using geographical information system based technique, *Air Pollution III. V.2, Air Pollution Engineering and Management*, eds. H. Power, N. Moussiopoulos & C. A. Brebbia, Comp. Mech. Publ., Southampton, pp. 447-454, 1995.

[135] Russell, G., McRae, G. & Cass, G.R., Mathematical Modelling of the Transport of Ammonium Nitrate Aerosol, *Atmospheric Environment*, **17**, pp. 949-964, 1983.

[136] Meixner, F.X., Franken, H.H., Duijzer, J.H. & Aalst, R.N., Deposition of HNO_3 to a pine forest, *Air Pollution Modelling and its Application VI*, Plenum Press, London, 1988.

[137] Kiselev, S.P., Ruev, G.A., Trunev, A.P., Fomin, V.M. & Schavaliev, M.S., *Shook-wave phenomena in two-component and two-phase flows*, Nauka, Novosibirsk, 261 p., 1992 (in Russian).

[138] Garland, J.A., Dry and wet removal of sulphur from the atmosphere, *Atmos. Environ*, **12**, pp. 349-362, 1978.

[139] Sehemel, G.A., Particle and gas deposition: a review, *Atmos. Environ*, **14,** pp. 983-1011, 1980.

[140] Piomelli, U., Balaras, E. & Pascarelli, A., Turbulent Structures in Accelerating Boundary Layers, *Journal of Turbulence*, **1**, pp. 1-16, 2000.

[141] *Hydrodynamic Instabilities and the Transition to Turbulence*. Topics in Applied Physics, Vol. 45, eds. H. L. Swinney & J. P. Gollub, Springer-Verlag, NY, 1981.

[142] Edward, O., *Chaos in Dynamic Systems*, Cambridge University Press, 1993.

[143] Mandelbrot, B.B. *The Fractal Geometry of Nature*, Freeman, NY, 1982.

[144] Paladin, G. & Vulpiani, A., Fractal Models of 2D and 3D Turbulence, *Fractals in Physics*, eds. L. Pietronero & E. Tosatti, Elsevier Science Publishers, pp. 624-631, 1986.

[145] Debnath, L., Wavelet transforms, fractals and turbulence, *Nonlinear Instability, Chaos and Turbulence*, Vol. I, eds. Lokenath Debnath & D. N. Riahi, WIT Press, pp. 129-196, 1999.

[146] Fletcher, C.A.J., *Computational Techniques for Fluid Dynamics, Vol. 1,2*, Springer Verlag, NY, 1988.

[147] Brebbia, C. A., *The Boundary Elements Method for Engineers*, London, 1978.

[148] Simpson, R.L., Agarwal, N.K., Nagabushana, K. A., Olcmen, S., Spectral Characteristics and Other Features of Separated Turbulent Flows, *AIAA Journal*, No3, pp. 446-452, 1990.

[149] Jigulev, V. N., Present State of Laminar Flows Stability Problem, *Mechanics of Turbulent Flows*, eds. V.V. Struminsky, Nauka, Moscow, pp. 109-133, 1980 (in Russian).

[150] Betchov, R., Transition, *Handbook of Turbulence*, Vol. 1, eds. W. Frost & T. H. Moulden, Plenum Press, NY, 1977.

[151] Riahi, D. N., *Flow Instability*, WIT Press, Southampton and Boston, 280 p., 2000.

[152] Tennekes, H. & Lumley, J. L., *A First Course in Turbulence*, MIT Press, Cambridge, Massachusetts, 1972.

[153] Hussain, A. K. M. F. & Reynolds, W. C., Measurements in fully development turbulent channel flow, *J. Fluid Ing.*, vol. 97, pp. 568-580, 1975.

[154] Perry, A. E., Lim, K. L. & Henbest, S. M., A Spectral Analysis of Smooth Flat-Plate Boundary Layers, *Proceedings of the 5th Symposium on Turbulent Shear Flows*, Springer-Verlag, New York, pp. 9.29-9.34, 1985.